35th Annual International Conference of the IEEE EMBS
Osaka, Japan, 3 - 7 July, 2013

Identification of a Parametric, Discrete-time Model of Ankle Stiffness.

Diego L. Guarin[1], *Student Member, IEEE*, Kian Jalaleddini[1], *Student Member, IEEE*, and Robert E. Kearney[1], *Fellow, IEEE*.

***Abstract*— Dynamic ankle joint stiffness defines the relationship between the position of the ankle and the torque acting about it and can be separated into intrinsic and reflex components.Under stationary conditions, intrinsic stiffness can described by a linear second order system while reflex stiffness is described by Hammerstein system whose input is delayed velocity. Given that reflex and intrinsic torque cannot be measured separately, there has been much interest in the development of system identification techniques to separate them analytically. To date, most methods have been nonparametric and as a result there is no direct link between the estimated parameters and those of the stiffness model. This paper presents a novel algorithm for identification of a discrete-time model of ankle stiffness. Through simulations we show that the algorithm gives unbiased results even in the presence of large, non-white noise. Application of the method to experimental data demonstrates that it produces results consistent with previous findings.**

I. INTRODUCTION

Joint stiffness can be defined as the dynamic relationship between the angular position of a joint and the torque acting about it [1]. It plays a vital role in the control of posture and is also important in the control of movement, since it determines the force required to execute a voluntary displacement [1].

Stiffness at the ankle can be described by the parallel cascade model shown in Fig. 1. Intrinsic stiffness is generated by the viscoelastic properties of the joint, passive tissue, and active muscle fibres. For small perturbations about a fixed operating point the intrinsic torque is described well by

$$T_i(t) = Ku(t) + Bv(t) + Ia(t), \tag{1}$$

where $u(t)$ is the joint angular position, $v(t)$ velocity, $a(t)$ acceleration and I, B and K are the inertial, viscous and elastic parameters respectively.

Reflex stiffness is generated by active muscle contraction in response to reflex activation from stretch receptors in the muscle. It can be described as a Hammerstein system with delayed velocity as the input. The input-output relation is given by

$$T_r(t) = \frac{g\omega^2}{s^2 + 2\zeta\omega s + \omega^2} f(v(t-\Delta)), \tag{2}$$

where g is the reflex gain, ω is the natural frequency, ζ the damping parameter, $f(\cdot)$ the static nonlinearity and Δ the delay.

[1]The authors are with the Biomedical Engineering Dept, McGill University. 3775, rue University, room 316 Montral, QC. H3A 2B4 Canada. Email: diego.guarinlopez, seyed.jalaleddini @mail.mcgill.ca and robert.kearney@mcgill.ca

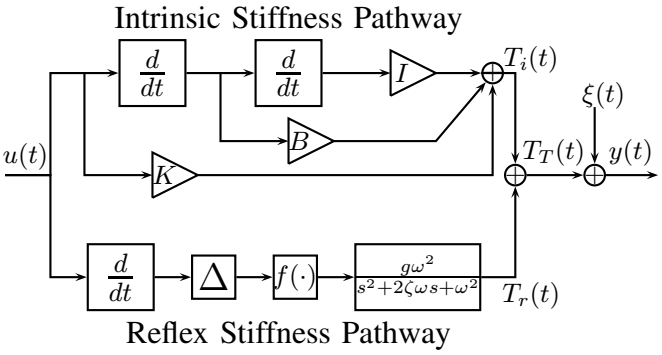

Fig. 1. Ankle stiffness model. Adapted from [1].

In practice is not possible to measure the intrinsic or reflexive torques separately, only their noisy sum can be measured [1]

$$y(t) = T_i(t) + T_r(t) + \xi(t) = T_T(t) + \xi(t), \tag{3}$$

where $T_T(T)$ is the total torque, $\xi(t)$ is a non-white noise signal [2] and $y(t)$ is the noisy measured torque.

Our laboratory has developed several system identification techniques to analytically separate the reflex and intrinsic torques from the measured total torque and position signals [1]–[3]. Many of these methods are nonparametric and model the linear dynamic elements using an Impulse Response Function (IRF). The major advantage of this is that little *a priori* information is required, typically only a upper bound of the system's memory length is needed. However, the disadvantage is that there is no direct relationship between the IRF estimate and the stiffness. Indeed, a second identification procedure involving a nonlinear minimization is required to link the IRF estimate to the parameters of Fig. 1.

In contrast, parametric methods require fewer parameters, and in the case of discrete-time models it is possible to link the discrete-time parameter estimates directly to the continuous-time parameters. The major disadvantage of this approach is that the system structure and order must be assumed *a prioir*.

A parametric method for ankle stiffness identification was presented by our laboratory some years ago [3], [4]. This method assumed that the shape of the nonlinearity was known and represented the linear elements of the intrinsic and reflex pathways by a multiple input single output autoregressive moving average model with exogenous input (MISO ARMAX). This paper presents a new iterative parametric method that improves on this previous work in two ways. First, the shape of the nonlinearity is estimated as part of the identification problem rather than being assumed *a priori*. Secondly, the linear element is represented as a MISO Box Jenkins model, a generalization of the ARMAX

structure, which has the advantage that the model parameter estimates are asymptotically independent of the noise model [5]. This means that given enough data the model parameter estimates will not be affected by the noise model. This is particularly important in physiological systems where noise is often composed of many components (e.g. electronic noise, low frequency drifts, unwanted philological signals, unmodeled dynamics). Thus, it is very advantageous to use identification methods which give unbiased results without requiring detailed noise models.

II. LINEAR DISCRETE TRANSFER FUNCTION MODEL

The first step in the development is to transform the nonlinear continuous-time model presented in Fig. 1 into a discrete-time transfer function model. To this end, the static non-linearity $f(\cdot)$ will be approximated by a linear combination of Tchebychev polynomials

$$\overline{v}(t-\Delta) = f(v(t-\Delta)) = \sum_{i=0}^{m} c_i \gamma_i[v(t-\Delta)]. \quad (4)$$

where γ_i is the ith Tchebychev polynomial and c_i is its weight.

Next, the linear element of the reflex stiffness will be transformed to a discrete-time model, using the bi-linear transformation, to give

$$T_r(k) = \frac{\kappa\left(1+2z^{-1}+z^{-2}\right)}{1+a_1 z^{-1}+a_2 z^{-2}}\overline{v}(k-\tau), \quad (5)$$

where z^{-1} is the backward shift operator, k is the discrete time, and τ is the discrete delay given by

$$\tau = \left\lceil \frac{\Delta}{T} \right\rceil,$$

where T is the sampling interval.

Substituting (4) in (5) gives

$$T_r(k) = \frac{1}{1+a_1 z^{-1}+a_2 z^{-2}} \sum_{i=0}^{m} \kappa_i \psi_i(k-\tau), \quad (6)$$

where

$$\begin{aligned} \kappa_i &= \kappa c_i, \\ v_i(k-\tau) &= \gamma_i[v(k-\tau)], \\ \psi_i(k-\tau) &= \left(1+2z^{-1}+z^{-2}\right) v_i(k-\tau). \end{aligned}$$

Finally, The total observed torque is given by

$$y(k) = Ku(k)+Bv(k)+Ia(k)+\frac{\sum_{i=0}^{m} \kappa_i \psi_i(k-\tau)}{1+a_1 z^{-1}+a_2 z^{-2}}+\xi(k). \quad (7)$$

Equation (7) is a linear transfer function model with terms having different denominators. The parameters to be identified are

$$\boldsymbol{\rho} = \left[K \;\; B \;\; I \;\; a_1 \;\; a_2 \;\; \kappa_0 \;\; \ldots \;\; \kappa_m\right]^T. \quad (8)$$

Note that neither κ, the gain of the linear element, nor the c_i, the polynomial coefficients, can be estimated explicitly, only their product is obtained. This reflects the uncertainty in the identification of any Hammerstein system where the gain may be partitioned arbitrarily between the nonlinearity and the linear dynamics.

The continuous-time and discrete-time parameters are related by

$$\hat{g} = -4\left(\frac{\hat{\kappa}}{\hat{a}_2+\hat{a}_1+1}\right), \quad (9a)$$

$$\hat{w} = \frac{2}{T}\sqrt{\frac{\hat{a}_1+\hat{a}_2+1}{\hat{a}_2-\hat{a}_1+1}}, \quad (9b)$$

$$\hat{\zeta} = -\frac{\hat{a}_2-1}{\left[\left(\hat{a}_2+1\right)^2-\hat{a}_1\hat{a}_1\right]^{1/2}}, \quad (9c)$$

where the "$\hat{}$" indicate estimates. The continuous-time reflex gain ($\hat{g}$) depends directly on the discrete-time reflex gain ($\hat{\kappa}$) but unfortunately, as noted above, this is not uniquely defined. Therefore, to provide a unique solution the following normalization condition will be imposed

$$\hat{\kappa} = \frac{1}{4}\left(\hat{a}_2+\hat{a}_1+1\right), \quad (10)$$

with the coefficients of the nonlinearity given by

$$\hat{c}_i = \frac{\hat{\kappa}_i}{\hat{\kappa}}, \quad i = 0, \ldots, m. \quad (11)$$

This normalization results in a value of $\hat{g} = -1$ so that all the gain of the reflex pathway will be assigned to the nonlinearity.

III. PARAMETER ESTIMATION

Equation (7) represents a mutiple-input, single-output (MISO) transfer function model, which for simplicity can be expressed as

$$y(k) = \frac{B_I(z^{-1})}{A_I(z^{-1})}u_I(k) + \frac{B_R(z^{-1})}{A_R(z^{-1})}u_R(k) + \frac{H(z^{-1})}{D(z^{-1})}e(k), \quad (12)$$

where $u_I(k)$ and $u_R(k)$ are the inputs to the intrinsic and reflexive pathways and

$$B_I(z^{-1}) = b_{I0} + b_{I1}z^{-1} + \cdots + b_{Im_I}z^{-m_I}, \quad (13a)$$

$$A_I(z^{-1}) = 1 + a_{I1}z^{-1} + \cdots + a_{In_I}z^{-n_I}, \quad (13b)$$

$$B_R(z^{-1}) = b_{R0} + b_{R1}z^{-1} + \cdots + b_{Rm_R}z^{-m_R}, \quad (13c)$$

$$A_R(z^{-1}) = 1 + a_{R1}z^{-1} + \cdots + a_{Rn_R}z^{-n_R}, \quad (13d)$$

$$D(z^{-1}) = 1 + d_1z^{-1} + \cdots + d_qz^{-q}, \quad (13e)$$

$$H(z^{-1}) = 1 + h_1z^{-1} + \cdots + h_qz^{-p}, \quad (13f)$$

define the filters associated with the models for the intrinsic stiffness, reflex stiffness and noise. The uncontrolled input $e(k)$ is assumed to be Gaussian white noise (GWN) with mean zero and variance σ^2.

The one-step ahead prediction of (12) is [6]

$$\hat{y}(k|k-1) = \frac{D}{H}\left[\frac{B_I}{A_I}u_I(k) + \frac{B_R}{A_R}u_R(k) + \left(\frac{H}{D}-1\right)y(k)\right], \quad (14)$$

where the notation (z^{-1}) has been dropped for simplicity. The prediction errors are given by

$$\begin{aligned}\epsilon(k) &= y(k) - \hat{y}(k|k-1) \\ &= \frac{H}{D}\left[y(k) - \frac{B_I}{A_I}u_I(k) - \frac{B_R}{A_R}u_R(k)\right].\end{aligned} \tag{15}$$

Now define a norm given by the sum of square errors

$$V(A_I, B_I, A_R, B_R, D, H) = \frac{1}{N}\sum_{k=1}^{N}\frac{1}{2}\epsilon(k)^2, \tag{16}$$

where N is the total number of elements. The objective of the identification is to determine the set of parameters $(A_I, B_I, A_R, B_R, D, H)$ that minimize the norm (16). This will occur when the partial derivatives of (16) w.r.t the parameters are equal to zero.

The partial derivatives of V with respect to the parameters of the intrinsic system are given by

$$\frac{\partial V}{\partial b_{Ii}} = \sum_k \left[A_I y_{If}(k) - B_I u_{If}(k)\right] u_{If}(k-i), \tag{17a}$$

$$\frac{\partial V}{\partial a_{Ii}} = \sum_k \left[A_I y_{If}(k) - B_I u_{If}(k)\right] \hat{x}_{If}(k-i), \tag{17b}$$

where

$$y_{If}(k) = \frac{D}{A_I H}\left[y(k) - \frac{B_R}{A_R}u_R(k)\right] = \frac{D}{A_I H}y_I(k), \tag{18a}$$

$$u_{If}(k) = \frac{D}{A_I H}u_I(k), \tag{18b}$$

$$\hat{x}_{If}(k) = \frac{D}{A_I H}\left[\frac{B_I}{A_I}u_I(k)\right] = \frac{D}{A_I H}\hat{x}_I(k). \tag{18c}$$

Here $\hat{x}_I(k)$ is an estimate of the contribution of u_I to the total output and the subscript f indicates that the signal was filtered by $D/(A_I H)$. The signal $\hat{x}_{If}(k)$ is known in the literature as instrumental variable [6], [7].

All the partial derivatives will be equal to zero when V is minimized. In consequence, equations (17) can be reformulated to be

$$0 = \sum_k \left[y_{If}(k) - \varphi_{If}^T(k)\theta_I\right] u_{If}(k-i), i = 1, \cdots, m_I, \tag{19a}$$

$$0 = \sum_k \left[y_{If}(k) - \varphi_{If}^T(k)\theta_I\right] \hat{x}_{If}(k-i), i = 1, \cdots, n_I, \tag{19b}$$

where

$$\begin{aligned}\varphi_{If}(k) = [&-y_{If}(k-1), \cdots, -y_{If}(k-n_I), \\ &u_{If}(k), \cdots, u_{If}(k-m_I)]^T,\end{aligned} \tag{20}$$

and

$$\theta_I = [a_{I1}, \cdots, a_{In_I}, b_{I0}, \cdots, b_{Im_I}]^T. \tag{21}$$

Equations (19a) and (19b) can be combined to give

$$0 = \sum_k \left[\hat{\varphi}_{If}(k) y_{If}(k) - \hat{\varphi}_{If}(k)\varphi_{If}^T(k)\theta_I\right], \tag{22}$$

where

$$\begin{aligned}\hat{\varphi}_{If}(k) = [&-\hat{x}_{If}(k-1), \cdots, -\hat{x}_{If}(k-n_I), \\ &u_{If}(k), \cdots, u_{If}(k-m_I)]^T.\end{aligned} \tag{23}$$

Rearranging (22) gives the estimator of (21) as

$$\hat{\theta}_I = \left[\sum_k \hat{\varphi}_{If}(k)\varphi_{If}^T(k)\right]^{-1}\left[\sum_k \hat{\varphi}_{If}(k) y_{If}(k)\right]. \tag{24}$$

A similar development for the reflex component gives the estimator of the reflex parameters:

$$\hat{\theta}_R = \left[\sum_k \hat{\varphi}_{Rf}(k)\varphi_{Rf}^T(k)\right]^{-1}\left[\sum_k \hat{\varphi}_{Rf}(k) y_{Rf}(k)\right], \tag{25}$$

were

$$\begin{aligned}\varphi_{Rf}(k) = [&-y_{Rf}(k-1), \cdots, -y_{Rf}(k-n_R), \\ &u_{Rf}(k), \cdots, u_{Rf}(k-m_R)]^T,\end{aligned} \tag{26a}$$

$$\begin{aligned}\hat{\varphi}_{Rf}(k) = [&-\hat{x}_{Rf}(k-1), \cdots, -\hat{x}_{Rf}(k-n_R), \\ &u_{Rf}(k), \cdots, u_{Rf}(k-m_R)]^T.\end{aligned} \tag{26b}$$

and

$$y_{Rf}(k) = \frac{D}{A_R H}\left[y(k) - \frac{B_I}{A_I}u_I(k)\right] = \frac{D}{A_R H}y_R(k), \tag{27a}$$

$$u_{Rf}(k) = \frac{D}{A_R H}u_R(k), \tag{27b}$$

$$\hat{x}_{Rf}(k) = \frac{D}{A_R H}\left[\frac{B_R}{A_R}u_R(k)\right] = \frac{D}{A_R H}\hat{x}_R(k). \tag{27c}$$

A. The identification problem

A similar procedure could be used to estimate the remaining elements of the system (H and D). However, the system and noise models are asymptotically independent thus is possible to set $D = H = 1$ and still obtain unbiased estimates of $\hat{\theta}_I$ and $\hat{\theta}_R$ [5], [7].

Another issue with this formulation is that, as may be seen in equations (18a) and (27a), $y_I(k)$ requires B_R and A_R to be known and, $y_R(k)$ requires B_I and A_I. Thus, $\hat{\theta}_I$ and $\hat{\theta}_R$ are interdependent. We propose to solve this problem using the following iterative algorithms. Note that the algorithm 1 calls the algorithms 2a and 2b during each iteration.

Algorithms 2a and 2b are similar to the Simplified Refined Instrumental Variable (SRIV) method proposed by Young [7], so it is appropriate to call algorithm 1 MISO SRIV.

TABLE I

SIMULATION RESULTS: VAF (%) BETWEEN PREDICTED TORQUES WITH DIFFERENT ALGORITHM AND NOISE-FREE TORQUES. SNR=10DB

	Intrinsic Torque			Reflex Torque			Total Torque		
	5th PCTL	50th PCTL	95th PCTL	5th PCTL	50th PCTL	95th PCTL	5th PCTL	50th PCTL	95th PCTL
MISO SRIV	99.6%	99.9%	99.9%	95.9%	97.9%	99.4%	99.4%	99.7%	99.9%
PC	96.5%	99.2%	99.9%	39.2%	86.9%	95.8%	96.5%	98.6%	99.6%
ARMAX	-	-	-	-	-	-	60.6%	81.2%	85.6%

Algorithm 1: Given y, u_R and u_I estimate $\hat{\theta}_I$ and $\hat{\theta}_R$.

1. Assume that $\hat{\theta}_R^0 = 0$. Set $y_I = y$ and compute $\hat{\theta}_I^0 = \left[\sum \varphi_I \varphi_I^T\right]^{-1} \left[\sum \varphi_I y_I\right]$. Set i=0.
2. Use $\hat{\theta}_I^i$ to compute $\hat{x}_I = \dfrac{B_I}{A_I} u_I$.
3. Compute $\hat{y}_R = y - \hat{x}_I$. Use $\hat{y}_R$, u_R and algorithm 2a to estimate $\hat{\theta}_R^{i+1}$.
4. Use $\hat{\theta}_R^{i+1}$ to compute $\hat{x}_R = \dfrac{B_R}{A_R} u_R$.
5. Compute $\hat{y}_I = y - \hat{x}_R$. Use $\hat{y}_I$, u_I and algorithm 2b to estimate $\hat{\theta}_I^{i+1}$.
6. Check whether $\hat{\theta}_I^{i+1}$ and $\hat{\theta}_R^{i+1}$ are significantly different from $\hat{\theta}_I^i$ and $\hat{\theta}_R^i$. If so, set i=i+1 and go to 2. Otherwise, terminate.

Algorithm 2a: Given y_R and u_R estimate $\hat{\theta}_R$

1. Compute $\hat{\theta}_R^0 = \left[\sum \varphi_R \varphi_R^T\right]^{-1} \left[\sum \varphi_R y_R\right]$. Set $j = 0$.
2. Using $\hat{\theta}_R^j$ compute y_{Rf}, u_{Rf} and $\hat{x}_{Rf}$.
3. Compute $\hat{\theta}_R^{j+1}$ using the current values of y_{Rf}, u_{Rf} and $\hat{x}_{Rf}$ and equations (26a), (26b) and (25).
4. Check whether $\hat{\theta}_R^{j+1}$ is significantly different from $\hat{\theta}_R^j$. If so, set j=j+1 and go to 2. Otherwise, terminate.

Algorithm 2b: Given y_I and u_I estimate $\hat{\theta}_I$

1. Compute $\hat{\theta}_I^0 = \left[\sum \varphi_I \varphi_I^T\right]^{-1} \left[\sum \varphi_I y_I\right]$. Set $j = 0$.
2. Using $\hat{\theta}_I^j$ compute y_{If}, u_{If} and $\hat{x}_{If}$.
3. Compute $\hat{\theta}_I^{j+1}$ using the current values of y_{If}, u_{If} and $\hat{x}_{If}$ and equations (20), (23) and (24).
4. Check whether $\hat{\theta}_I^{j+1}$ is significantly different from $\hat{\theta}_I^j$. If so, set j=j+1 and go to 2. Otherwise, terminate.

IV. SIMULATION

The algorithm was evaluated using a challenging but realistic scenario in which the reflex contribution to the noisy total torque power was small (10 %). The continuous-time model shown in Fig. 1 was simulated using Simulink. Noise was added to the simulated output with amplitude adjusted to give a SNR of 30dB and 10dB. The noise signal was designed to have characteristics similar to those observed experimentally. Thus it was the sum of a GWN simulating electronic noise ($\sigma = 0.08$), a 1Hz low-pass filtered Gaussian signal to simulate physiological noise ($\sigma = 0.5$) and, a 60 Hz sinusoidal to simulate ambient noise ($\sigma = 0.03$). The position input was a pseudo random multi level sequence whose switching rate was selected from a random variable with uniform distribution with values between 200 and 300 ms [8]. The inputs used were samples of those used experimentally (see Fig 3a). Each simulation was run for 60 s at 1 kHz and then decimated to 200 Hz for analysis. A set of 100 realizations were simulated using a new input and noise signals in each realization.

A. Results

The identification results obtained with the MISO SRIV method were compared to those given by the nonparametric parallel-cascade (PC) algorithm described by Kearney, et. al. [1] and the parametric ARMAX method introduced by Kukreja, et. al. [3]. Some initial remarks are necessary: First, the PC method is nonparametric, so there is no direct link between the identified parameters and the ankle stiffness model parameters. Therefore, we compared the algorithms on the basis of their predictive ability measured in terms of the Variance Accounted For (%VAF) between the torques (predicted by a free-run of the estimated model) and the noise-free simulated torques. Second, the ARMAX method does not yield independent estimates of the intrinsic and reflex torques, so only the total torque can be compared.

Table I presents the %VAFs obtained for the different algorithms. The probability densities of the %VAFs were not Gaussian therefore results are presented as the 5th, 50th and 95th percentiles (PCTL) observed in the 100 simulations.

The PC and MISO SRIV algorithms gave similar results for intrinsic torque. Median %VAF was close to 100% in booth cases, although with the MISO SRIV algorithm the 90% range (the difference between the 95th and 5 PCTLs), a measure of the spread of the distribution, was somewhat smaller (3.4% compared to 0.3%). There was a large difference between the PC and the MISO SRIV algorithms for reflex torque. The median %VAF with the nonparametric method was fairly good (86.9%) but the 90% range was large (55.5%). In contrast, the MISO SRIV algorithm had a better median %VAF (97.9%) and much lower 90% range (4%). Finally, when it comes to the total torque there was not much difference between the PC and the MISO SRIV algorithms (due to the relatively small contribution of the reflex torque) but, the results with the new algorithm were slightly superior.

The ARMAX method gave the worst results; the median %VAF was significantly lower and had the highest 90% range (25% compared to 3.1% with the PC and 0.5% with the MISO SRIV methods).

Given the excellent predictive ability of the MISO SIRV method we next examined how well it estimated the para-

TABLE II

SIMULATION RESULTS: ESTIMATION OF THE PARAMETERS. SNR= 10DB

	K	B	I	a_1	a_2	Reflex Gain
True	50	1.65	0.0152	-1.952	0.955	4
Estimated	49.9	1.73	0.0145	-1.952	0.955	4.2
SD	1.6	0.02	0.0004	0.004	0.004	0.5

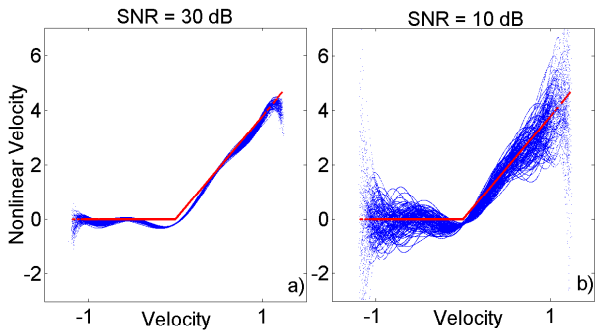

Fig. 2. Simulation Results: Estimation of the nonlinearity shape for 100 simulations (blue lines), true nonlinearity shape (red line). a) SNR = 30 dB, b) SNR = 10 dB.

meters. Table II shows that the expected values of both $\hat{\theta}_I$ and $\hat{\theta_R}$, for the 100 simulations, were very close to the true values and the SD of each parameter were small compared with the mean values. The reflex gain was computed as the slope of the nonlinearity by fitting a straight line between the appropriate points.

Fig 2 presents the true shape of the nonlinearity (half-wave rectifier, red lines) and the shapes estimated for the differet simulation runs with the MISO SRIV algorithm (blue lines). At high SRN (Fig 2a) the algorithm captured well the nonlinearity, but as the SNR decreased there was more variability (Fig 2b). Even so, the %VAF was not greatly affected.

B. Discussion

There were three main findings of the simulation study. First the MISO SIRV provides the best prediction of the three methods. Second, it gives unbiased estimate of the discrete parameters even in the presence of large amounts of colored noise. Thirdly, it captures the shape of the nonlinearity well. The high accuracy of the reflex parameters estimates is remarkable given that the effective SNR for the reflex torque was very low since the intrinsic torque acts as an additional noise signal. Indeed, the effective SNR was -20dB for the case of 10dB of additive noise. It can also be noted that the estimated elastic (B) and intrinsic (I) parameters are slightly bias. This probably happened because those parameters are very small compared to K.

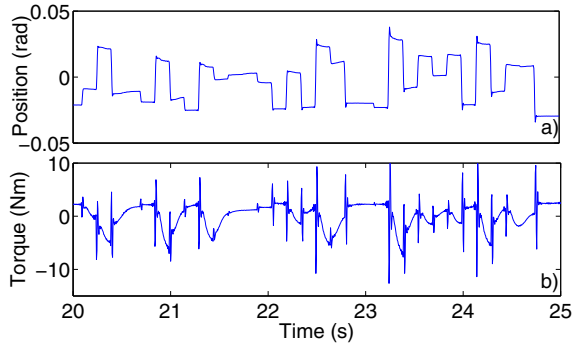

Fig. 3. a) Position input and b) total torque recorded during one experiment. Ankle position: + 0.2 rad.

TABLE III

REAL DATA RESULTS: ESTIMATION OF THE CONTINUOUS-TIME PARAMETERS FOR DIFFERENT ANKLE POSITIONS

	-0.2 rad	-0.1 rad	0 rad	+0.1 rad	+0.2 rad
$\hat{K}$	27.8	28.9	29.7	44.8	49.5
$\hat{B}$	0.79	0.80	0.80	0.74	0.76
$\hat{I}$	0.016	0.016	0.012	0.017	0.017
$\hat{\omega}$	16.1	15.8	15.6	14.8	13.6
$\hat{\zeta}$	0.65	0.62	0.62	0.65	0.62
Reflex Gain	6.9	6.9	11.3	14.3	18.1
RC	9.3 %	11.9 %	24.7 %	26.4 %	30.8 %
$\text{VAF}_{\text{MISO SRIV}}$	92.8 %	91.3 %	87.5 %	90.5 %	87.1 %
VAF_{PC}	94.1 %	93.5 %	85.9 %	91.3 %	88.3 %

V. APPLICATION TO EXPERIMENTAL DATA

The algorithm was also validated with experimental data. The subject lay supine with the left leg immobilized and the foot attached firmly to a pedal connected to a hydraulic actuator. The subject pushed slightly on the pedal to generate an average torque equal to 5% of maximum platarflexing voluntary contraction. The same input used in simulations was applied to the ankle through the actuator. Ankle position and torque were sampled at 1000 Hz for 75 s and then decimated to 200 Hz for analysis. Trials were performed at five different position: neutral position (0 rad), two plantar flexed positions (-0.1 rad and -0.2 rad), two dorsiflexed positions (+0.1 rad and +0.2 rad). Subjects were instructed to maintain a constant level of contraction and not to react to he perturbations. Fig. 3 shows a small segment of the position input (panel a) and the total torque (panel b) recorded during one trial.

These data were used to estimate ankle stiffness using both the MISO SIRV and the PC methods. The first half of each trial was used for estimation and the last half for validation.

A. Results

Table III shows the %VAF between the measured and predicted torque with the PC and the MISO SRIV algorithms for the validation data. The %VAF was high ($\geq$ 85.9%) for both methods at all positions indicating that both models described that data well.

The elasticity (K) and the reflex gain (the slope of the nonlinearity) changed the most. Both increased when the ankle was moved from plantarflexion to dorsiflexion. The relative reflex contribution (RC) to the total measured torque was lowest (9.3%) in the most plantarflexed positions and largest (30.8%) at the most dorsiflexed positions.

The natural frequency ($\hat{\omega}$) decreased slightly as the ankle was moved from plantarflexion to dorsiflexion. Other parameters showed no consistent trend.

The shape of the nonlinearity is not shown but was similar to a half-wave rectifier in all the trials.

B. Discussion

The experimental data demonstrated that both intrinsic and reflex contributions increased significantly when mean ankle positions was moved from plantarflexion to dorsiflexion. These results are consistent with what has been reported previously [9]. It is interesting to note that the intrinsic

stiffness was almost constant when the ankle moved from plantarflexion to neutra position but increased substantially when it was moved from neutral position to dorsiflexion. This is consistent with previous findings which have shown that K is more or less constant in the midrange.

VI. CONCLUSIONS

We have presented a new iterative algorithm based on the minimization of prediction error approach for identification of parallel-cascade model of ankle stiffness. Simulations demonstrated that this algorithm estimate the parameters of the ankle stiffness model accurately even when the contribution of the reflex torque was very low. Further, a pilot experimental study demonstrated that it produces results consistent with previous findings.

The advantage of this algorithm compared with similar methods is that it yields accurate results even in the presence of colored noise and that it gives a direct estimate of the parameters of the model with low variance.

It should be noted that under some conditions reflex dynamics required a third order dynamics [9]. The MISO SRIV algorithm can be extended to test this hypothesis simply by increasing the order of the filters $B_R(z^{-1})/A_R(z^{-1})$ appropriately. This will be pursuit in a future study.

REFERENCES

[1] R. E. Kearney, R. B. Stein, and L. Parameswaran, "Identification of intrinsic and reflex contributions to human ankle stiffness dynamics," *IEEE Trans. on Biomedical Eng*, vol. 44, no. 6, pp. 493 – 504, 1997.

[2] Y. Zhao, D. T. Westwick, and R. E. Kearney, "Subspace methods for identification of human ankle joint stiffness," *IEEE Trans. on Biomedical Eng*, vol. 58, no. 11, pp. 3039 – 3048, 2011.

[3] S. L. Kukreja, H. L. Galiana, and R. E. Kearney, "Narmax representation and identification of ankle dynamics," *IEEE Trans. on Biomedical Eng*, vol. 50, no. 1, pp. 70 – 81, 2003.

[4] D. L. Guarin and R. E. Kearney, "A narmax method for the identification of time-varying joint stiffness," in *Engineering in Medicine and Biology Society (EMBC), 2012 Annual International Conference of the IEEE*, 2012, pp. 6518 –6521.

[5] D. A. Pierce, "Least squares estimation in dynamic-disturbance time series models," *Biometrika*, vol. 59, no. 1, pp. 73 – 78, 1972.

[6] L. Ljung, *System Identification - Theory For the User*, 2nd ed. Upper Saddle River, N.J.: Prentice Hall, 1999.

[7] P. C. Young, *Recursive Estimation and Time-Series Analysis*. Berlin: Springer, 2011.

[8] K. Jalaleddini and R. E. Kearney, "Estimation of the gain and threshold of the stretch reex with a novel subspace identication algorithm," in *Engineering in Medicine and Biology Society (EMBC), 2011 Annual International Conference of the IEEE*, 2011, pp. 4431 – 4434.

[9] M. Mirbagheri, H. Barbeau, M. Ladouceur, and R. Kearney, "Intrinsic and reflex stiffness in normal and spastic, spinal cord injured subjects," *Exp Brain Res*, vol. 141, no. 4, pp. 446 – 459, 2001.